Advances in Concrete Construction, *Vol. 7, No. 1 (2019) 23-30*
DOI: https://doi.org/10.12989/acc.2019.7.1.023

Design of small impact test device for concrete panels subject to high speed collision

Sanghee Kim[a], Seung Yong Jeong[b] and Thomas H.-K. Kang[*]

Department of Architecture and Architectural Engineering, Seoul National University, Seoul, 08826, Korea

(Received November 4, 2018, Revised December 18, 2018, Accepted December 19, 2018)

Abstract. Five key items were used to create an economical and physically small impact test device for concrete panels subject to high speed collision: an air-compressive system, carbon steel pipe, solenoid valve, carrier and carrier-blocking, and velocity measurement device. The impact test device developed can launch a 20 mm steel spherical projectile at over 200 m/s with measured impact and/or residual velocity. Purpose for development was to conduct preliminary materials tests, prior to large-scale collision experiments. In this paper, the design process of the small impact test device was discussed in detail.

Keywords: small impact test device; impact resistance; high speed collision; concrete panel

1. Introduction

Fragments or projectiles ejected due to various causes such as mechanical collisions, explosions, and shootings poses a threat to the safety of people, buildings, equipment, and objects nearby. When a high velocity projectile collides with a target, local damage to the target due to penetration, scabbing on rear face, perforation, or cracking often occurs. For safety sake, determination of impact resistance and damage done to such targets is necessary. Various impact test devices have been used by researchers depending on purpose and need (Fig. 1). Test devices used to evaluate the impact resistance of concrete and other materials for protection can be divided into two types: the first, being the 'shooting' method, whereby gas or gunpowder is employed as a propellant to launch a projectile, and the second, called the 'drop-weight' method, where mass or elevation of an object is used.

In this study, a shooting method was selected so that the strain rate of materials could be reflected (Almusallam *et al*. 2015, Hong and Kang 2016, Li *et al*. 2016, Kim *et al*. 2017, Chen *et al*. 2018). Although it is easy to generate kinetic energy by increasing the weight or height through the drop-weight method, it is difficult to produce a high strain rate. Therefore, this design process entailed the development of a small impact test device that is capable of launching a projectile at high speed.

(a) Nitrogen gas gun test device, Chungnam National University (Lee *et al*. 2018)

(b) Canon (Lee *et al*. 2013)

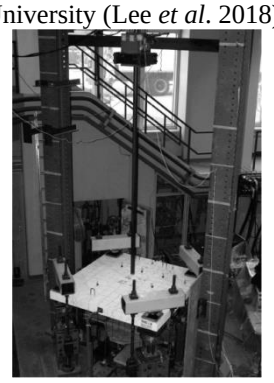

(c) Drop-weight test device (Hrynyk and Vecchio 2014)

(d) Compressed Nitrogen and Helium gas gun test device (Soe *et al*. 2013)

Fig. 1 Various impact test device types

2. Design concept

2.1 Key ideas for small impact test device

For the evaluation of the impact resistance of concrete through observation of the collision of a projectile traveling at high velocity, the design of an impact test device is being presented. The focus in development is on reduction in size to existing examples of large impact test equipment. Given the laboratory environment and research topic, three parameters/goals were held in the development of the small impact test device - namely: 1) Fit in an area of roughly 5,000×1,500 mm; 2) Ability to launch a 20 mm steel ball at a rate of more than 300 m/s, and 3) Be capable to launch projectiles of various sizes and shapes semi-permanently

∗Corresponding author, Professor
E-mail: tkang@snu.ac.kr
[a]Ph.D.
[b]Ph.D. Student

ISSN: 2287-5301 (Print), 2287-531X (Online)

(a) Air-compressor (www.dewalt.com)

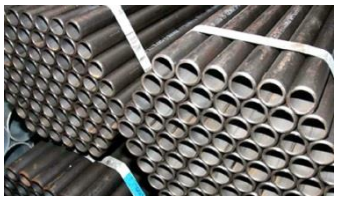

(b) Carbon steel pipes for pressure service (www.sinhwasteel.com)

(c) Solenoid valve (www.electricsolenoidvalves.com)

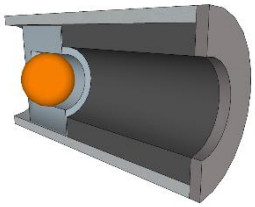

(d) Carrier and carrier-blocking

(e) Commercial velocity measurement (www.competitionelectronics.com)

Fig. 2 Key equipment for small impact test device development

and economically.

In order to satisfy parameters outlined above, utilization of five key components shown in Fig. 2 were selected to meet the installation site requirement of 5,500×1,500 mm. An air-compressor (Fig. 2(a)) was adopted to minimize the use of consumables, which are akin to elevation of cost of operation, such a gunpowder or nitrogen gas, along with ready-made carbon steel pipes to serve as a barrel (Fig. 2(b)). Since the importance to provide sufficient air pressure from an air tank to the projectile in the barrel instantly cannot be over emphasized, a push button commercial available electronic solenoid (Fig. 2(c)) that allows the valve to be opened for a brief moment was utilized. To load projectiles of various sizes and shapes within the barrel, a carrier, in the form of a cartridge, was designed to launch the projectile along with a carrier-blocking to stop the cartridge prior to the projectiles collision with the test object (Fig. 2(d)). After the carrier-blocking, the projectile proceeds forward under its own inertia. A velocity measurement device (Fig. 2(e)) can be employed. Measurement of velocity is a critical factor in evaluating the impact resistance of a test object. A commercial available velocity measurement device was used for the sake of both economics and convenience.

2.2 Overall plan

The overall design concept for the impact test device is

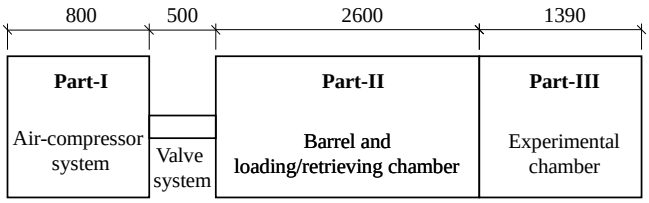

Fig. 3 Overall design concept for small impact test device (unit: mm)

as shown in Fig. 3. A space of 1,000 × 800 mm was reserved for the air compressor and air tank to be installed in Part-I. The air compressor and air tank generate the force necessary to accelerate the test projectile or flying object. The length of the valve system between the air tank and the barrel was set at 500 mm, considering the size of the solenoid valve and the union required to connect to Part-I and -II. In Part-II, an area 2,600 mm in length was reserved for the barrel along with the loading and retrieving chamber for the projectile. Since the experimental chamber in Part-III required space for velocity measurement instrument(s) as well as test specimens, the area set aside was determined to be 1,390 mm long by 500 mm wide.

3. Air-Compression system design

3.1 Design of air-compressor and air tank capacity

Instead of nitrogen or gunpowder used in the design of other impact test device systems, the decision was made early in the process to use an air-compressor to create the energy needed to launch test projectiles. The reason for this decision, in addition to the cost in purchasing nitrogen or gunpowder, was that nitrogen pressure equipment is considerably bulky and requires a great deal of additional equipment, whereas gunpowder presented difficulties in terms of handling. An air-compressor, on the other hand, required only a small area to install and made it possible to use the device semi-permanently without incurring any additional costs. The pressure of the air compressor was chosen at 2 MPa. Greater pressure would have required placement of a special order making the component more expensive. The safety control box for the air compressor, which is required to be installed, limited pressure to an upper bound of 1.75 MPa.

The air-compressor compresses air into the air-tank, which is then discharged through the barrel as soon as the solenoid valve is opened. For the purpose of estimating the velocity of the projectile, it is important to determine how much pressure the air-tank can hold up to the end of the barrel. If the pressure difference between the air-tank and the end of the barrel is significant, the projectile will not be launched at full velocity. Therefore, reducing the pressure difference between the tank and the barrel end is an important aspect of tank capacity design. The required capacity of the air-tank is calculated using Boyle's law (Eq. (1)). Herein, $P_{initial}$ is the initial pressure of the air in the air-tank (MPa); $Vol_{initial}$ is the initial volume of the air in the air-tank (L); $P_{changed}$ is the total change in pressure in the

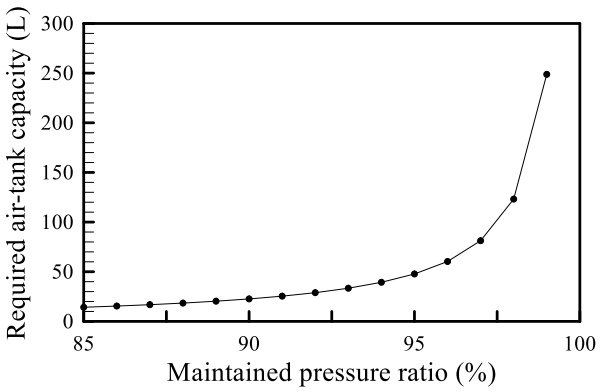

Fig. 4 Predicted pressure ratio and tank capacity relationship

Fig. 5 Manufacturing air compressor and air tank system

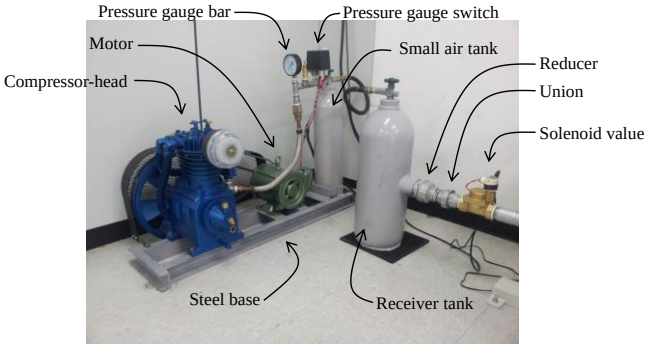

Fig. 6 Details of air compressor system

air-tank and the barrel (MPa), and $Vol_{chanaed}$ is the total changed volume of the air in the air-tank and the barrel (L).

$$P_{initial}Vol_{initial} = P_{changed}Vol_{changed} \quad (1)$$

The relationship between the pressure ratio of the end of barrel to the air tank and tank capacity is shown in Fig. 4, where the diameter and length of the barrel were assumed to be 20 mm and 2000 mm, respectively. A 20L air tank was selected as the receiver tank due to the limited space available and need to fill reservoir air tank quickly for continuous experiments. The 20 L air tank had a diameter of 249 mm and length of 510 mm.

The purpose and goal of the air compressor and air tank were discussed with a specialist wherein based on experience and additional information provided by the manufacture several solid ideas regarding the solenoid value, receiver tank, and installation of a safety device were put into effect. The safety device is a pressure control switch that serves to stop air compressing if the air pressure in the tank exceeds a pre-set amount. To operate the air compressor more efficiently and reliably, adaptation for a three-phase electric power source as suggested by the specialist was also implemented.

3.2 Construction of air-compression system

The compressor head and motor were installed on a steel base along with the air tank, which also served as the pressure control tank (Fig. 5). After connecting the pressure control switch to the inlet of the air tank, a bar pressure gauge and a check valve were connected to the left side of the small air tank. The check valve was installed to prevent the backflow and permit airflow in one direction only. On the right side of the small tank, a receiver tank was installed. The compressor-head, small tank, and the receiver tank were then connected via a hose.

A hole with a diameter of 65 mm was then drilled in the middle of the receiver tank, and a pipe with an inner diameter of 65 mm and length of 100 mm was welded to it. Since the diameter of the connecting pipe was 65 mm and the inside diameter of the barrel was 40 mm, a reducer was used for the connection. Since it was difficult to disassemble the reducer following installation, a union was installed in between the reducer and the solenoid valve to facilitate easier assembly and disassembly. Finally, the solenoid valve was connected to the barrel via the union, with the receiver tank, reducer, union, and solenoid valve all installed in a straight line (Fig. 6). The air-compressor, motor, and small air tank were then set upon the steel base. To equalize the receiver tank and barrel altitude from the floor level, a rubber plate was used, placed beneath the receiver tank.

4. Barrel design

4.1 Barrel size and details

The size of the barrel is determinable given pressure and capacity of the air tank. The velocity of the projectile can be calculated using both the acceleration formula (Eq. (2)) and the uniformly accelerated motion formula (Eq. (3)), Eq. (4) can be derived from Eqs. (2)-(3). Herein, a is the acceleration (m/s^2); V_{start} is the initial velocity of the projectile while within the loading chamber (m/s); V_{out} is the projectile velocity at the barrel's end (m/s); t is the duration (sec), and s is the displacement (m). Considering Newton's second law (Eq. (5)) of motion and the initial velocity of zero (V_{start} = 0 m/s), Eq. (6) is obtainable. Herein, F_p is the force applied to the projectile (N), and M_p is the mass of the projectile (kg). Finally, the speed of the projectile at the end of barrel is determined, as shown in Eq. (7). The end of the barrel and the test object are in close

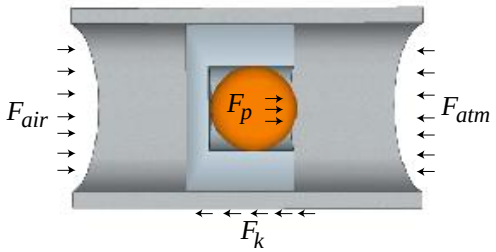

Fig. 7 Free body diagram of projectile

proximity, so it can be held that there is no loss of velocity due to air resistance. Therefore, the projectile velocity at the barrel`s end is equal to the impact velocity.

$$a = \frac{(V_{out} - V_{start})}{2t} \tag{2}$$

$$s = V_{start}t + \frac{V_{out} - V_{start}}{2} = V_{start}t + t \times \frac{at}{2} = V_{start}t + \frac{at^2}{2} \tag{3}$$

$$2as = V_{out}^2 - V_{start}^2 \tag{4}$$

$$F_p = M_p a \tag{5}$$

$$V_{out}^2 = 2 \times \left(\frac{F_p}{M_p} \right) \times s \tag{6}$$

$$V_{out} = V_{imp} = \sqrt{2 \times s \times \frac{F_p}{M_p}} \tag{7}$$

In Eq. (7), the values of s and M_p are known, while the value of F_p is unknown. Therefore, the value of F_p must be defined in order to obtain the precise velocity of the projectile. In physics, a free body diagram of a projectile is graphically illustrated with the active force acting upon the projectile (F_p). This is exemplified here with the air-tank force (F_{air}), atmospheric force (F_{atm}), and frictional force (F_k), as shown in Fig. 7. The equilibrium equation of the three forces is given in Eq. (8). Because lubricant was used in the course of the experiments, the coefficient of friction is 0.06, with the judgment that there was no friction. The atmospheric pressure is 0.1 MPa, while the atmospheric force is the $0.1 \times A_{in,barrel}$ (N), where $A_{in,barrel}$ is the inner cross sectional area of the barrel (mm^2). The value of F_p can be obtained via Eq. (9). The barrel size can be calculated from Eqs. (10)-(11). In order to achieve a velocity of 300 m/s, F_p requires 738 N. Since the acting pressure on the projectile is 1.6 MPa, along with the assumption that the inner barrel diameter is 20 mm, the internal cross-sectional area of the barrel capable of receiving a force of 738 N is 462 mm^2 (Eqs. (12)-(13)). In other words, if the inner diameter of the barrel is 24.2 mm or greater, the projectile can be launched at a speed of 300 m/s or more (Eq. (14)). Herein, $d_{in,barrel}$ is the inner diameter of the barrel (mm) and $r_{in,barrel}$ is the inner radius of the barrel (mm). For this reason, a carrier of 24.2 mm in diameter or larger is required to mount a projectile 20 mm in diameter.

$$F_p = F_{air} - F_{atm} - F_k \tag{8}$$

Table 1 Carbon steel pipes for pressure service (KS D 3562 (Korea Agency for Technology and Standards 2018)) and expected velocities

Nominal Diameter (mm)	Outer diameter (mm)	Nominal wall thickness (mm)			Weight of carrier (g)	Expected velocity (m/s)
		Sch. 20	Sch. 40	Sch. 60		
25	34	-	3.4	3.9	10	257
32	42.7	-	3.6	4.5	31	269
40	48.6	-	3.7	4.5	61	272
50	60.5	3.2	3.9	4.9	114	271
65	76.3	4.5	5.2	6.0	206	260

$$F_p = (F_{air} - 0.1) \times A_{in,barrel} = (1.6 \text{ MPa}) A_{in,barrel} \tag{9}$$

$$F_p = \frac{V_{out}^2}{2s} \times m = 1.6 A_{in,barrel} \tag{10}$$

$$F_p = \frac{(300\,m/s)^2}{2 \times (2m)} \times (0.0328\,kg) = 1.6 A_{in,barrel} \tag{11}$$

$$1.6 A_{in,barrel} = 738 \text{ N} \tag{12}$$

$$A_{in,barrel} = 462 \text{ mm}^2 \tag{13}$$

$$d_{in,barrel} = 24.2 \text{ mm} \, (r_{in,barrel} = 12.1 \text{ mm}) \tag{14}$$

The barrel diameter size can be chosen from among manufactured carbon steel pipes for pressure service, in accordance with KS D 3562 (Korea Agency for Technology and Standards, 2018). When the barrel pressure is 1.75 MPa, a Sch 20 or greater is required.

Given the initial design concept to launch a spherical projectile with a diameter of 20 mm and the need for the inner diameter of the barrel to equal and/or exceed 24.2 mm in order to achieve a speed of 300 m/s or more, a carrier capable of carrying the spherical projectile is required. The weight of the carrier, as well as expected velocity, is shown in Table 1. Considering the difficulty in achieving a launch speed of 300 m/s, a 40A-Sch.40 pipe was selected, which offers the highest expected speed.

Within the barrel from the loading chamber to retrieving chamber, the carrier and projectile move linearly together due to the acting pressure. The carrier stops at the end of the barrel as a function of the carrier-blocking, while only the projectile moves forward to the target specimen due to inertia (Fig. 8). In order to stop the carrier at the end of the barrel, a carrier-blocking that features a reduced inner cross-sectional area of the end of the barrel was also manufactured (Fig. 7). The inner diameter of the carrier-blocking was set to 25 mm so that the projectile can pass through smoothly. The carbon steel pipe for a pressure of 40A-Sch.40 was finally selected in consideration of the area of contact between the carrier and the carrier blocking, as well as the inner diameter of the carrier blocking (Fig. 8). The carrier-blocking was manufactured by cutting a circular steel pipe with an outer diameter of 40 mm, thickness of 7.5 mm, an inner diameter of 25 mm, and a length of 50 mm. It was then placed at the end of the barrel and welded to the

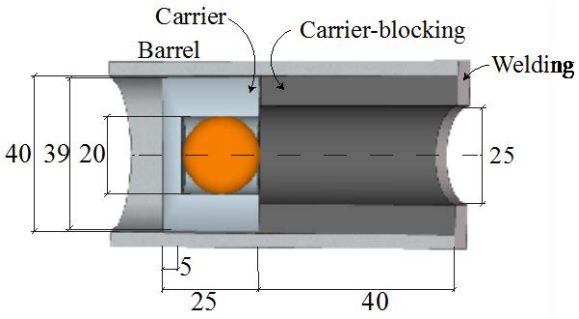

Fig. 8 Details of the carrier and carrier-blocking device (unit: mm)

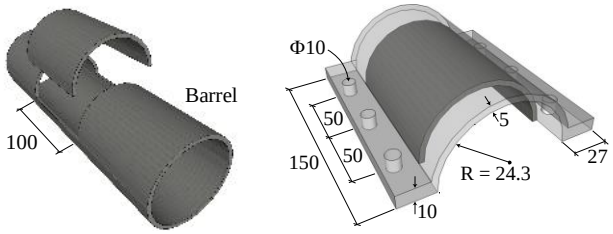

(a) Cutting the half pipe (b) Loading chamber cover details

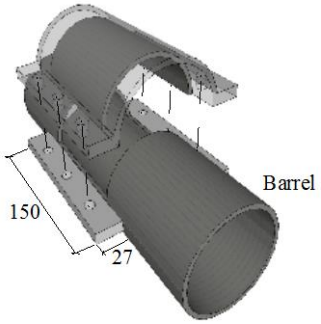

(c) Details of the wings of loading chamber

(d) Assembled cover and wings

Fig. 9 Loading chamber and retrieving chamber (unit: mm)

carbon steel pipe. In order to reduce the weight of the carrier given that the heavy and long carrier could decrease the launching velocity of the projectile, the projectile was composed of aluminum. Detailed dimensions, as shown in Fig. 8, were: 39 mm outer diameter, 20 mm inner diameter, and 20 mm inner depth. The weight of the carrier was 61 g. The total weight of the carrier and the steel spherical projectile combined was 92.8 g.

The loading and retrieving chambers were made the same in the shape shown in Fig. 9. Each pair has an axial length of 100 mm and was cut at a distance of 200 mm from the ends of the barrel (Fig. 9(a)). The loading/retrieving chamber cover was made by welding the part cut from the barrel, as well as an additional semi-circular steel plate with wings having 6 screw holes (Fig. 9(b)). The thickness of the

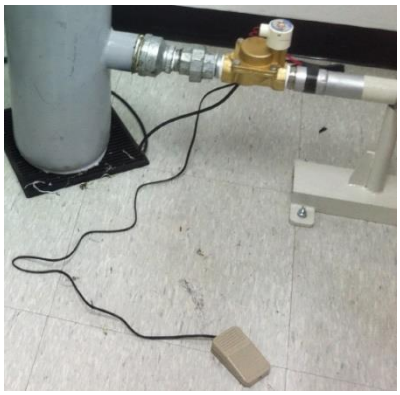

Fig. 10 Foot button and solenoid valve

semi-circular steel plate is 5 mm, with a radius of 24.3 mm. The thicknesses and width of the wings welded to the semi-circular steel plate are 10 mm and 27 mm, respectively. The wings are also attached to the barrel as shown in Fig. 9(c). Each wing has three threaded holes with a diameter of 10 mm, allowing the loading/retrieving chamber cover and barrel to be bolted together. The distance between the holes is 50 mm. The bolts used had a diameter of 8 mm and a length of 40 mm (Fig. 9(d)). A sealant was applied to the cover in order to prevent air from leaking from the gap between the barrel and the cover.

The inner surfaces of the ready-made carbon steel pipes for pressure service were not smooth, so a honing process was conducted first. The essence of the honing process is the use of an abrasive stone to scrub the inner surface to produce a smooth high-precision surface. This abrasive process helps the carrier and the projectile pass through the inner barrel and enhances velocity.

4.2 Solenoid valve

A solenoid valve is a device that automatically opens and closes, allowing the transfer of air from the air-tank into the barrel. When using the solenoid valve, no additional cost is incurred, as well as being easy to employ. The solenoid valve is located between the air-tank and the barrel, connecting them. The size of the valve is determined by the barrel, which was determined to have an inner diameter of 40 mm. Thus, the inner diameter of solenoid valve was also 40 mm. The selected type of switch is a foot-button with a long lead wire, facilitating easy turning of the solenoid value (Fig. 10).

5. Experimental chamber design

The chamber encompasses the space where the projectile is set to collide with the test object. Within the chamber, it is necessary to have an appropriate space for velocity measurement along with a space for installation of the test object(s) and beyond for when projectile passes through the test object. Experiments were planned for testing two concrete panel specimens, one 400×400 mm and the other 200×200 mm. The initial chamber was thus designed accordingly. The size of the chamber was

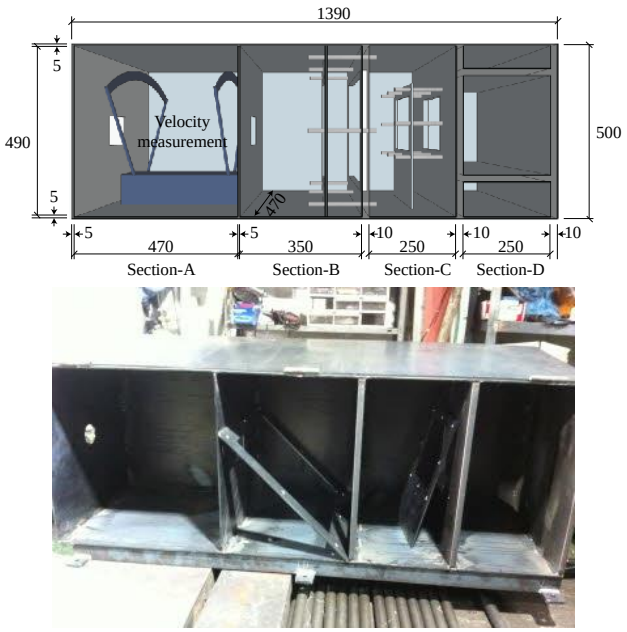

Fig. 11 Illustrations and production of chambers (unit: mm)

1,390×500×470 mm (length×height×depth), and the space was separated into four rooms as depicted in Fig. 11. Section-A was used for installing an impact velocity measurement device. Here, the Competition Electronics ProChrono Digital, with dimensions of 400×100×80 mm and a velocity measurement range of 6 to 2100 m/s, was used with an accuracy of +/1% (https://www.competitionelectronics.com). Given that the length of the velocity measurement is approximately 400 mm, 35 mm of marginal space was added to both sides. Therefore, the total length of Section-A was 470 mm. Section-B was for installing a 400×400 mm concrete panel specimen. Section-C was for installing a 200×200 mm concrete panel specimen. Section-D was for installing other various types of specimens. This section also serves as a room for receiving any projectile which exits the concrete test panels and/or fragments by scabbing failure.

In order to produce the main experiment chamber, five outer walls and three inner partition walls were cut and welded accordingly (Fig. 11). One more outer wall was cut for the door. The door and main chamber were connected by a set of three hinges. A door handle was welded at the lower middle portion of the door. The left outer wall was drilled with a hole, and the barrel was inserted into this hole. The completed barrel and the main experimental chamber were painted white.

The barrel and experimental chambers were designed to be made at a factory. The tri-clamp pipe clamp and H-channel (Fig. 12) were added during assembly of the barrel and the experimental chamber. The tri-clamp pipe clip was welded at the end of the supporter with a tri-clamp pipe clip gripping the barrel to prevent it from moving. The H-channel was used to anchor the barrel to the floor using anchor bolts and supports.

6. Installation and modification of impact test device

(a) Tri-clamp pipe clip (www.walmart.ca)

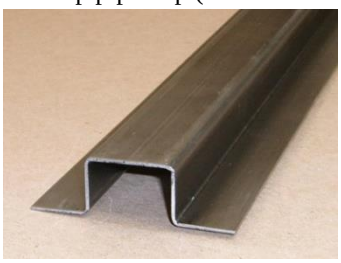

(b) H-channel (mpmetals.com)

Fig. 12 Tri-clamp pipe clip and H-channel for installing barrel

Fig. 13 Installation of impact test device

6.1 Installation of impact test device

The manufactured air compressor system, barrel, and main experimental chamber were assembled in the laboratory (Fig. 13). The H-channel and the main experimental chamber were anchored to the floor with the use of anchor bolts. Next, the air compressor system and barrel were connected, followed by a rubber plate which was laid under the tank to match the height of the receiver tank and the barrel. A foot button was installed for operation of the solenoid valve. Finally, the three-phase electric power source was connected to the motor.

6.2 Modification of impact test device

Originally, there was no plan for measuring the residual velocity of the projectile. However, residual velocity was determined to be an important factor in evaluating the impact resistance of test objects in view of the law of conservation of energy. Therefore, Sections-C and -D were combined to provide space for installing a second velocity measurement. To test both the 200×200 mm and the 400×400 mm concrete panel specimens, holes were drilled in each of the back steel frames to accommodate connecting bolts. The modified experimental chamber was now divided into Sections-A, -B and -E as shown in Fig. 14.

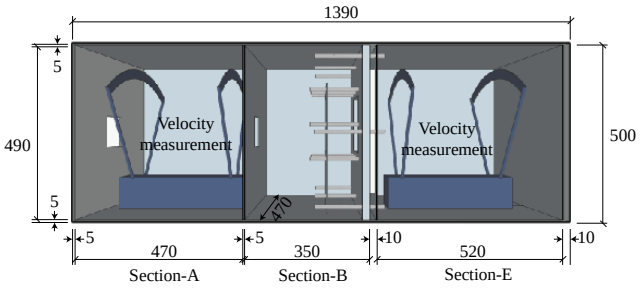

Fig. 14 Modification of chamber (unit: mm)

Numerous breathing holes were drilled in the door panel of the chamber as shown in Fig. 15. These holes were added to allow air to exit quickly without accumulation. Before adding the breathing holes, the door to the chamber opened and closed with a bang due to the rapid change in pressure associated with air in the barrel when the projectile was launched.

In the initial test of the device, the aluminum carrier was damaged due to impact which had not been considered in the design process. The impact stress on the carrier exceeded the allowable stress (55 MPa) of aluminum (AL 6061-O) (Eqs. (15)-(16)). Where, $\sigma_{\max}$ is the maximum compressive stress of the carrier (MPa); M_p is the weight of the projectile (kg); V_{imp} is the impact velocity of the projectile (m/s); $E_{carrier}$ is Young's modulus of the carrier (MPa); $A_{carrier}$ is the cross-sectional area of the carrier (mm^2), and $l_{carrier}$ is the length of the carrier (mm). An additional device was required to provide protection for the carrier. A 40 mm length of PCV pipe was used to protect the carrier instead of installing additional equipment. Placing a PCV pipe in front of the carrier-blocking helped facilitate carrier energy dissipation.

$$\sigma_{\max} = \sqrt{\frac{M_p V_{imp}^2 E_{carrier}}{A_{carrier} l_{carrier}}} \tag{15}$$

$$\sigma_{\max} = 244 > 55 \text{ MPa} \tag{16}$$

7. Further research

Experimental equipment was manufactured and tested. Measured average velocities of 225 m/s with 1.75 MPa pressure in the air-tank were recorded. Measured velocities were approximately 50 m/s lower than initially planned. Explanation being the possibility of consumption of thermal energy through the object and a 1 mm gap through which power was lost between the barrel and the air pressure valve. When calculating F_p, atmospheric pressure was used to determine the resistance force on the carrier and the projectile. However, the drag force can become heightened when the velocity of the projectile exceeds 0.5 Mach, a speed at which the air can be considered a compressible fluid, drastically increasing its drag coefficient (Munson *et al.*, 1990; Vennard and Street, 1982). Since the target speed was 300 m/s (0.88 Mach) in this study, this effect should be considered.

Fig. 15 Breathing holes

In development of this study, a piece of plastic pipe was used to protect the aluminum carrier and the end-block within the barrel from high-energy impact forces imposed when the carrier was launched. The plastic component, which had a length of 30 mm, protected the end-blocking. However, the tip of the barrel tilted slightly downward as the tests were continuously conducted. As a result, the projectile struck the lower portion of the test specimens rather than the center. Further studies are deemed necessary in order to ensure that the barrel tip does not tilt downward. The possibility to place a pedestal beneath the barrel or utilize an alternate material that is capable of separating the carrier and the projectile in a manner similar to end-blocking exists.

8. Conclusions

In order to launch the spherical steel ball at over 300 m/s, as defined in the original plan, the design process of the small impact test device for the evaluation of the impact resistance of the target object was introduced in detail for each part, within the plan. Due to limited physical space and budget, the design of the experimental equipment utilized mostly compact parts and inexpensive components. Based on the design, manufacture and trial tests, the following conclusions were drawn:

- The air tank capacity is an important aspect in maintaining air-pressure from the solenoid valve to the end of the barrel. It is critical in determining the exit velocity of the projectile. The larger the size of the air tank, the higher maintained air-pressure, and thus higher speed of the projectile. However, for this study, a 20 L tank was used given prescribed space limitations. A small air tank was installed to refill the receiver tank, to allow continuous experiments to be conducted rapidly. The pressure in the air-tank was set at 1.75 MPa, in accordance with safety rules and capacity of the pressure control box.
- The velocity of the projectile can be calculated using the acceleration formula, as well as the uniformly accelerated motion formula. Given conditions known at this time, the equation can be derived from the relationship between velocity and the force imposed by the projectile. Forces acting upon the projectile and the

carrier were identical to the pressure of the tank after subtracting atmospheric pressure. Therefore - if the inner diameter of the barrel is known, the launching speed of the projectile can be predicted. The required inner diameter of the barrel to achieve the design speed exceeded 24 mm, and a carrier was needed for the delivery of the 20 mm projectile from the loading chamber to the retrieving chamber. Due to weight of the carrier, expected velocity was predicted to be as low as 272 m/s. However, measured average velocity for the tests was 225 m/s, approximately 50 m/s lower than the expected velocity. Reasons for loss in velocity could include and be attributed to consumption of thermal energy, increase in drag coefficient, and/or loss of air pressure due to gaps.

• The experimental chamber was originally divided into four sections, consisting of: a front section for impact velocity measurement of the projectile, a second section for installing the 400×400 mm concrete panel specimen; a third section for installing a 200×200 mm concrete panel specimen, and a fourth section to receive the projectile, or test irregular shaped specimens. In order to measure residual velocity of the projectile, the experiment chamber was modified into three sections. These sections were the impact velocity measurement section, specimen installation section, and the residual impact velocity measurement section. Also, breathing holes were drilled in the experiment chamber to release compressed air within the barrel when the projectile was launched.

Acknowledgments

The work presented in this paper was funded by National Research Foundation of Korea (NRF) grants (NRF-2018M2A8A4083866). The views expressed are those of the authors, and do not necessarily represent those of the sponsor.

References

Almusallam, T.H., Abadel, A.A., Al-Salloum, Y.A. and Siddiqui, N.A. (2015), "Effectiveness of hybrid-fibers in improving the impact resistance of RC slabs", *Int. J. Impact Eng.*, **81**(1), 61-73.

Chen, X., Chen, C., Liu, Z., Lu, J. and Fan, X. (2018), "Compressive behavior of concrete under high strains after freeze-thaw cycles", *Comput. Concrete*, **21**(2), 209-217.

Hong, S. and Kang, T.H.K. (2016), "Dynamic strength properties of concrete and reinforcing steel subject to extreme loads", *ACI Struct. J.*, **113**(5), 983-995.

Hrynyk, T.D. and Vecchio, F.J. (2014), "Behavior of steel fiber-reinforced concrete slabs under impact load", *ACI Struct. J.*, **111**(5), 1213-1224.

Kim, S., Kang, T.H.K. and Yun, H.D. (2017), "Evaluation of impact resistance of steel fiber-reinforced concrete panels using design equations", *ACI Struct. J.*, **114**(4), 911-921.

Korea Agency for Technology and Standards, (2018), *Carbon Steel Pipes for Pressure Service KS D 3562:2018*, Korea Standards Association, 123. (in Korean)

Lee, S., Cho, S.S., Jeon, J.E., Kim, K.Y. and Seo, K.S. (2013), "Impact analyses and tests of concrete overpacks of spent nuclear fuel storage casks", *Nucl. Eng. Technol.*, **46**(1), 73-80.

Lee, S., Kim, G., Kim, H., Son, M., Choe, G. and Nam, J. (2018), "Strain behavior of concrete panels subjected to different nose shapes of projectile impact", *Mater.*, **11**(3), 1-15.

Li, J., Wu, C., Hao, H., Su, Y. and Liu, Z. (2016), "Blast resistance of concrete slab reinforced with high performance fibre material", *J. Struct. Integrit. Mainten.*, **1**(2), 51-59.

Munson, B.R., Rothmayer, A.P. and Okiishi T.H. (2012), *Fundamentals of Fluid Mechanics*, 7th Edition, John Wiley & Sons, Inc.

Soe, K.T., Zhang, Y.X. and Zhang, L.C. (2013), "Impact resistance of hybrid-fiber engineered cementitious composite panels", *Compos. Struct.*, **104**, 320-330.

Vennard, J.K. and Street, R.L. (1982), *Elementary Fluid Mechanics*, 6th Edition, Wiley.

CC